Applied SEISMOLOGY

A Comprehensive Guide to Seismic Theory and Application

By
Mamdouh R. Gadallah
and
Ray L. Fisher

PennWell®

Contents

List of Figures

List of Tables

Caption and Courtesy List

Fig. 1–1 Seismic Waves from Big Bertha's Firing
Fig. 1–2 Dip Shooting
Fig. 1–3 Typical 2-D Seismic Geometry
Fig. 1–4 Continuous or Single-fold Subsurface Coverage
Fig. 1–5 CMP Shooting
Fig. 1–6 Multi-fold Shooting
Fig. 1–7 Meandering Stream Channel
Fig. 1–8 3-D Prospect Layout

Fig. 2–1 A Fossil Sequence
Fig. 2–2 Dating Rocks from Fossils
Fig. 2–3 Internal Structure of the Earth
Fig. 2–4 The Lithosphere
Fig. 2–5 Mountains, Ridges, and Rises of the World
Fig. 2–6 Seafloor Spreading
Fig. 2–7 Mantle Convection Currents
Fig. 2–8 Tectonic Plate Boundaries
Fig. 2–9 Tectonic Plate Model
Fig. 2–10 Pangea, the Universal Continent, about 200 Million Years Ago
(modified from R.S. Dietz and J.C. Holden, Scientific American, *1970)*
Fig. 2–11 The Continents in Their Present Positions and Their Projected Positions 50 Million Years from Now
(After R.S. Dietz and J.C. Holden, Scientific American, *1970)*
Fig. 2–12 Top Part of the Earth's Crust
Fig. 2–13 Formation of Igneous Rocks
Fig. 2–14 The Rock Cycle
Fig. 2–15 Sorting
Fig. 2–16 Prevalent Sedimentary Rock Types
Fig. 2–17 The East Texas Oil Field
Fig. 2–18 Strike and Dip
Fig. 2–19 Strike, Dip, and Plunge
Fig. 2–20 Stress-strain Relationship
Fig. 2–21 Types of Stress
Fig. 2–22 Folding of Rocks
Fig. 2–23 Monoclines, Synclines, and Anticlines
Fig. 2–24 Terms Describing Anticlines
Fig. 2–25 Symmetric and Asymmetric Folds
Fig. 2–26 Anticlinal Dome, Overhead View
Fig. 2–27 Eroded Folds
Fig. 2–28 An Eroded, Plunging Syncline in Northwest Africa *(Photo by U.S. Air Force)*
and an Eroded, Plunging Anticline in the Zagros Mountains of Iran
(Photo by Aerofilms, Ltd., through courtesy of John S. Shelton)
Fig. 2–29 Joints
Fig. 2–30 Fault Motion
Fig. 2–31 Dip Slip Faults
Fig. 2–32 Well Bores through Normal and Reverse Faults
Fig. 2–33 Fault Displacement along the Great Glen Fault
Fig. 2–34 Horsts and Grabens
Fig. 2–35 Rollover Anticline
Fig. 2–36 The Fuel Cycle
Fig. 2–37 Molecular Forms of Petroleum
Fig. 2–38 Migration of Hydrocarbons
Fig. 2–39 Components of Clastic Sedimentary Rocks
Fig. 2–40 The Oil Window
Fig. 2–41 Effect of Grain Size on Porosity and Permeability
Fig. 2–42 Geothermal Gradient in Sedimentary Basins

1 Overview and Summary

Introduction

Until 1859, petroleum exploration was a rather simple and straightforward procedure. One simply looked for oil seepage at the surface—particularly near streams and from oil springs. Petroleum was used principally for medicinal purposes at that time, so the approach yielded a sufficient supply to meet demands.

In 1859, Colonel E. L. Drake completed the first successful well, drilled specifically for oil (although wells drilled earlier for other purposes had yielded oil). Actually, Drake used the early method of petroleum exploration since his well was located near a known oil seep along Oil Creek in western Pennsylvania. Soon, there were many wells being drilled up and down Oil Creek.

These early successes led to an exploration method often called *creekology* in which accumulations of oil were associated with low spots along and near streams. Hills and plateaus were not considered suitable drilling sites.

Trendology was another early exploration method arising from the observation that oil pools and fields frequently occurred along almost straight lines for many miles. In other words, after early discovery of two or more fields, lines connecting these were extended in both directions and wells located along the line. Actually, this is a relatively sound procedure, which is still used under certain conditions. Locating wells near oil seeps is also a good method.

Intergranular porosity can result from original spaces between grains at the time of deposition remaining after lithification or from fractures after lithification. Solution cavities in limestones can produce interconnected pores or voids that allow fluid flow through the reservoir rock. Table 2–4 lists classifications of rock porosity and Table 2–5 gives classifications of permeability.

Table 2–4 *Reservoir Rock Porosity*

Ranges of Values	Description
0 to 5%	Negligible
5 to 10%	Poor
10 to 15%	Fair
15 to 20%	Good
20 to 25%	Very Good
greater than 25%	Excellent

Table 2–5 *Reservoir Rock Permeability*

Ranges of Values	Description
less than 0.1 to 1 md	Poor
1 to 10 md	Fair
10 to 100 md	Good
100 to 1000 md	Very Good
greater than 1000 md	Excellent

Reservoir rock porosity is either primary, with the remainder of the original spaces between sand grains and particles or fossil pieces, or secondary, meaning it was formed after deposition and burial. Secondary porosity results from solution in *fossil molds* (or vugs) and from fractures, such as between crystals in limestone and dolomite. Porosity may be measured by visual examination of well cuttings taken from core samples, a standard laboratory procedure, or from wire-line well logs.

In deep reservoirs, as cementation and compaction increase, porosity and permeability decrease. Gas reservoirs occur at greater depths but require less porosity and permeability to be productive.

Reservoir rock permeability indicates how easily fluids can flow through a rock and thus, depends on interconnection of the pores. Permeability is measured using a *perm plug*, a cylindrical piece of rock drilled from a core. Tight sands and limestone have permeabilities of less than 5 md.

Source rocks are sedimentary rocks in which organic matter is preserved. Black sediments have high organic content. Coals are preserved woody material. Black shales have 1 to 5% organic matter. They are the most common source rock.

Generation, migration, and accumulation of petroleum. Methane (swamp gas) is generated at shallow depths via biogenic or bacterial activity. However, this methane is generated at too shallow a depth for large quantities to be trapped. (Some efforts are being made to capture such gas produced at municipal landfills.) Bacterial action decreases with increasing depth and temperature.

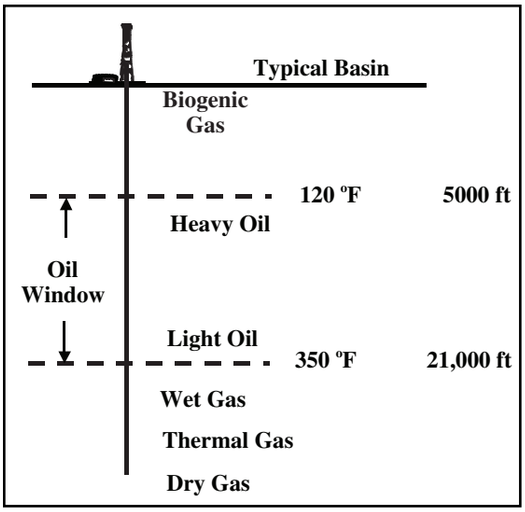

Fig. 2–40 *The Oil Window*

Crude oil is generated very slowly, taking millions of years at temperatures of from 120°F to 350°F. Heavy oils with low API gravity are generated at the lower temperatures in this range. (Heavy oil may be biodegraded lighter oil.) Light oils are generated at the higher temperatures in the range. Thermal gas is generated at temperatures above 350° F. At these temperatures crude oil breaks down into graphite (C) and gas.

Organic matter and coal generate gas. Wet gas with associated condensate is generated at shallower depths. Dry gas with no liquids is generated at deeper depths.

The oil window (Fig. 2–40) is the subsurface region of oil generation. The temperature range of 120°F to 350°F corresponds to a depth range of about 5000 ft (1524 m) to 21,000 ft (6400 m). Heavy oil is generated at the top of the oil window and light oil at the bottom. Similarly, wet gas is generated just below the oil window and dry gas at deeper depths.

The reason for the differences in type of petroleum generated at different depths and temperature ranges becomes clear when the nature of heat is investigated. Heat is actually molecular motion. The higher the temperature, the faster the molecules move. The larger the hydrocarbon molecule, the less stable it is at high temperatures. Thus temperature establishes a ceiling on molecular size.

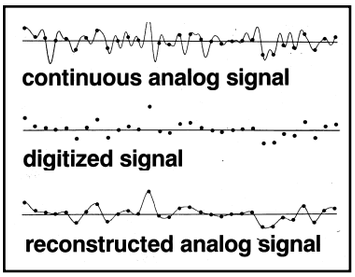

Fig. 3–25 *Digital Recording*

In most cases, the ability to correctly reconstruct a digital signal depends upon the frequency content of the signal and the sampling increment.

Figure 3–26 shows the effect of sampling at different *sample increments* or *sample periods*. In Figure 3–26a, the input is a 25-Hz sinusoid. The reconstructions of the outputs sampled at 2 ms, 4 ms, and 8 ms are the same as the input. In Figure 3–26b, the input is a 75-Hz sinusoid. The reconstructions of the outputs sampled at 2 ms and 4 ms are the same as the input, but the output sampled at 8 ms is a 25-Hz sinusoid! In Figure 3–26c the input is a 150-Hz sinusoid. The reconstruction of the output sampled at 2 ms is the same as the input, but the 4 ms output is a 100-Hz sinusoid and the 8 ms output is a 25-Hz sinusoid!

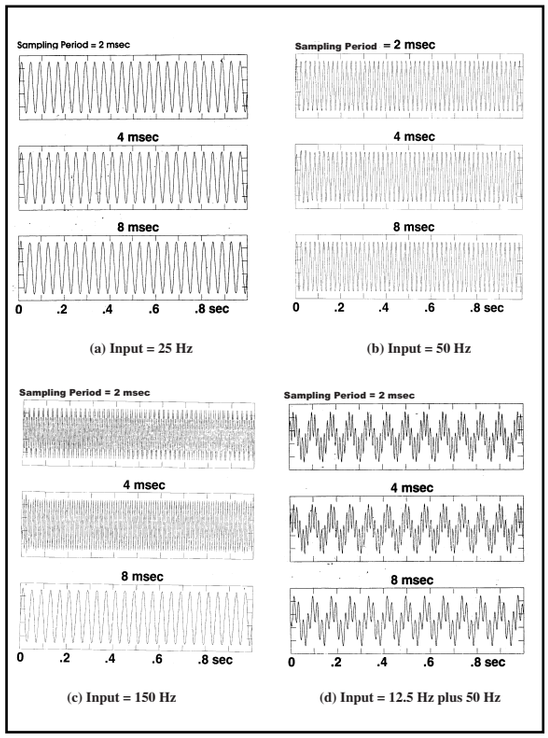

Fig. 3–26 *Effect of Sample Period*

In Figure 3–26d, the input is the sum of 12.5-Hz and 75-Hz sinusoids but the reconstructed output is the sum of 12.5 and 25-Hz sinusoids. What is being demonstrated here is the phenomenon called *aliasing*.

The *Sampling Theorem* can be stated as follows:

An analog signal which is band-limited to frequencies less than f_0 is completely described by samples taken at intervals of time Δt, where $\Delta t < 1/2f_0$. Conversely, then, an analog signal band-limited to signals less than f_0 can be completely recovered from samples taken at intervals of time Δt, if $f_0 < 1/2\Delta t$. If, however, a signal sampled at a sample interval Δt contains frequencies higher than $f_N = 1/2\Delta t$, where f_N is the Nyquist or alias frequency, it cannot be correctly recovered (using conventional processing techniques) because of a distortion called aliasing.

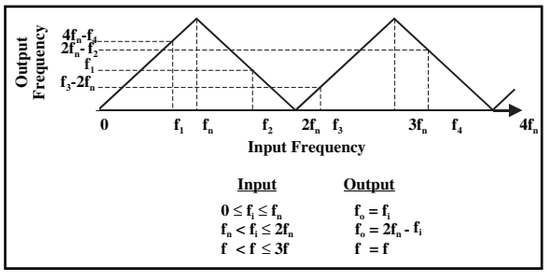

Fig. 3–27 *Aliasing*

Analyzing the data of Figure 3–26, it can be seen that the 25-Hz sinusoid is below Nyquist for all three sample periods. The 75-Hz signal is lower than f_N for 2 and 4 ms sampling but above f_N for 8 ms sampling. From Table 3–3, the Nyquist frequency for 8 ms is 62.5 Hz and 75 Hz is 12.5 Hz more than f_N. The output frequency f_o is 50 Hz or 12.5 Hz less than f_N.

Table 3–3 *Nyquist Frequency*

DT (ms)	f_N (Hz)
0.5	1000
1	500
2	250
4	125
8	62.5

At 4 ms sampling, the 150-Hz sinusoid is 25 Hz above f_N and its output of 100 Hz is 25 Hz below f_N. At 8 ms sampling, the 150-Hz sinusoid is 87.5 Hz above f_N or and 25 Hz above $2f_N$. Its output of 25 Hz is equal to the difference between the input and $2f_N$. Figure 3–27 is a chart for calculating output frequencies relative to input and multiples of f_N.

To prevent aliasing, a filter must be applied before sampling or resampling to a larger sample period, and a filter must be applied to limit frequencies to below Nyquist.

5. Complete Table 3–7 by determining the output frequencies for each input frequency and sample period.

Table 3–7 *Output Frequencies for Various Sample Periods*

Input Frequency (Hz)	Frequency Output (Hz)	Frequency Output (Hz)	Frequency Output (Hz)	Frequency Output (Hz)
60				
120				
180				
240				
300				

6. Given the impulse response of a system shown in Figure 3–72, what is the output when the input is as shown in the following?

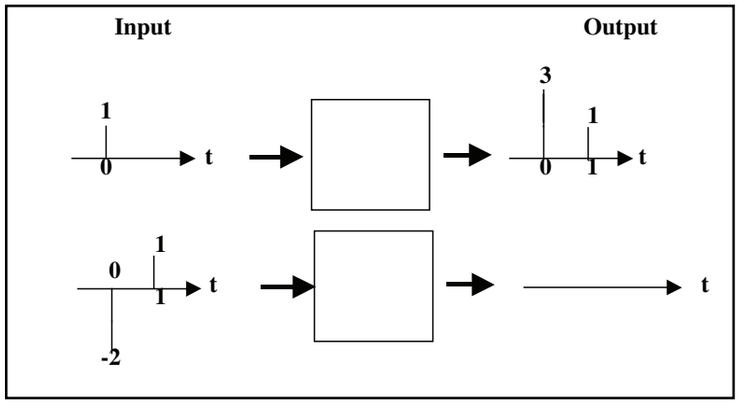

Fig. 3–72

7. Given wavelet $a = \{5, -2\}$ and wavelet $b = \{-3, 1\}$, calculate the cross-correlations, ϕab and ϕba.

8. Calculate the autocorrelation of wavelet a in exercise 7.

9. Which of the following are minimum-phase wavelets? The first value in each case is at time zero.

   a. 6, -1. –2

   b. 3, 4, -4

   c. 0, 12, -1, -6

   d. –2, 5, -2

   e. 28, -27, 5

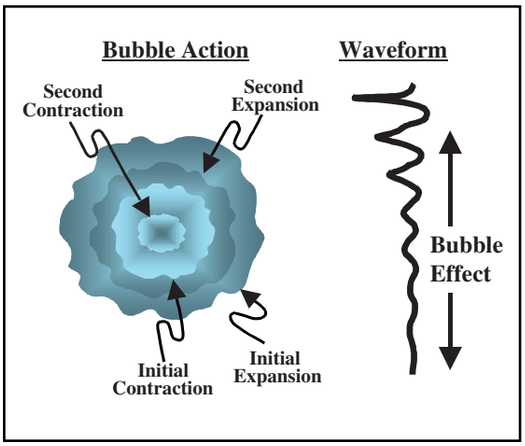

Fig. 5–26 *The Bubble Effect*

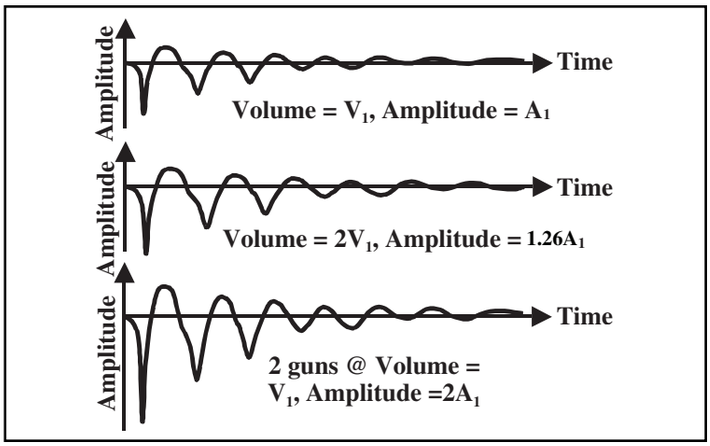

Fig. 5–27 *Airgun Pressure–Volume Relationship*

pressure is once again higher than water pressure and a second, although smaller, expansion occurs. Repeated contractions and expansions occur until all the energy is dissipated. Figure 5–26 illustrates this and the waveform produced by the bubble effect.

Pressure produced by a single airgun is proportional to the cube root of *gun volume*—the total space in the airgun occupied by air. Signal amplitudes are proportional to pressure, so amplitude is also proportional to $V^{1/3}$. So, as shown in Figure 5–27, increasing the volume of a single airgun gives only 26% larger amplitude. However, using two airguns of the same volume placed closely together produces twice the amplitude.

Airguns are used in arrays for two reasons—to increase signal amplitudes and to minimize the bubble effect. The latter is illustrated in Figure 5–28. In this very simple array, three different size guns (different volumes) are used—one large gun, three medium size guns, and three small guns. The guns of the same size are grouped closely together (clustered). Spacing between the one large gun and the two clusters is such that the bubbles interfere destructively except at the initial expansion. Note that the airguns in the array do not fire simultaneously. The smaller guns are delayed because their bubbles achieve maximum expansion earlier than the larger guns. Note also the lower frequency content of the larger guns. Large numbers of airguns of various sizes are grouped together to form tuned arrays. With proper spacing of single guns and gun clusters (array design), virtually any desired signal waveform can be achieved.

The two main objectives of airgun array design are to obtain adequate energy source strength and sufficiently broad frequency bandwidth. The best way to determine a source strength requirement is to conduct a field experiment using different strength sources to record a 2-D line and then process and analyze the results. For the obvious reasons (time and cost), this is almost never done. A review of previously acquired 2-D or 3-D data can aid in determining adequate source strength requirements. Amplitude decay analysis and time variant spectral analysis of previously gathered 2-D or 3-D data can help determine the depth (recording time) of penetration of useful seismic energy. It is possible to *overshoot* an area by using an energy source that is too strong.

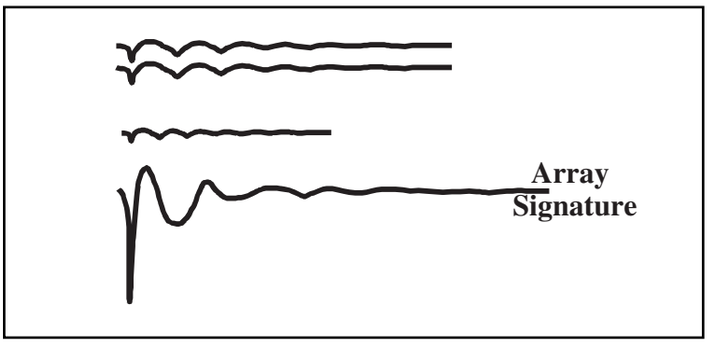

Fig. 5–28 *Waveform Synthesis by Airgun Arrays*

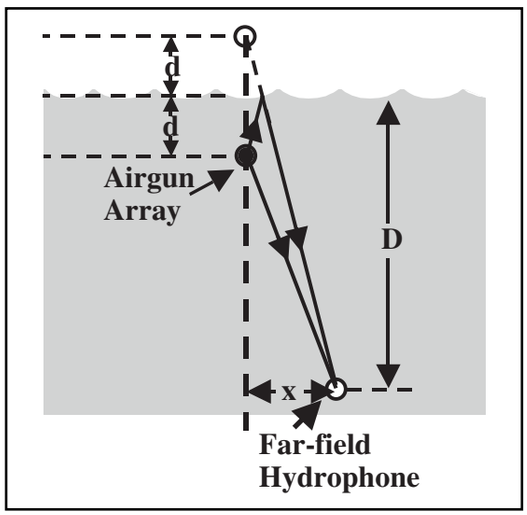

Fig. 5–29 *Measurement of the Far-field Signature*

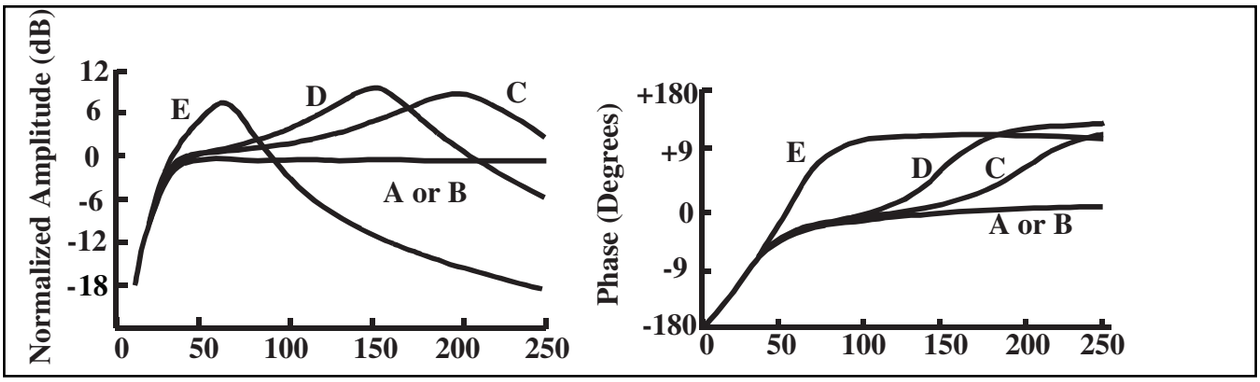

Fig. 5–74 *Effect of Geophone Planting Conditions on Amplitude and Phase Responses*

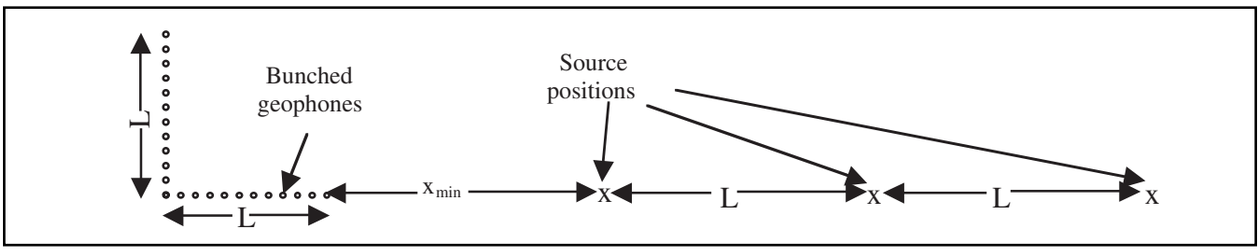

Fig. 5–75 *Noise Spread and Shooting Procedures*

thunder, surf, earthquakes) or cultural (vehicular and foot traffic, grazing animals, pumps). *Source-generated* noise includes ground roll, air blast, guided waves, and others. Since noise is undesirable, although unavoidable, measurement of noise characteristics (frequency, wavelength propagation velocity) aids in design of techniques to minimize noise recording. Such measurements are done in noise tests.

A useful method of conducting noise tests is to lay out about 12, or more, groups of several bunched geophones, with total length L, and a similar set of 11 geophones perpendicular to these. The length L should be equal to the planned group interval in the seismic survey. Figure 5–75 shows the suggested layout and shooting procedure. Shoot (or sweep) into these geophones starting at the minimum offset x_{min} and continuing at intervals L as shown in Figure 5–75. The minimum offset should also be equal to that planned for the survey. One record is made at each source position. Offsets for the first record are x_{min} *to* x_{min}+ L. Offsets for the second record are x_{min}+L *to* x_{min}+ $2L$, etc. Records are combined with traces offset-ordered.

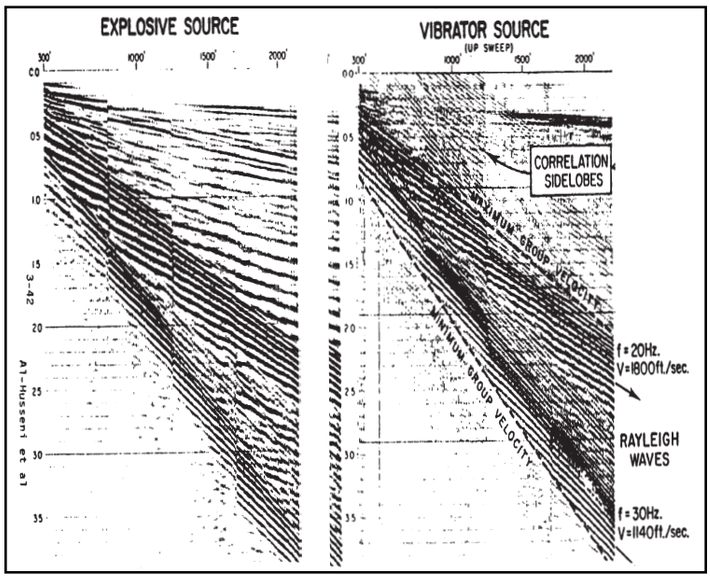

Fig. 5–76 *Noise Test Example*

Figure 5–76 is an example of a noise test record. It is important in conducting noise tests that the same source be used as in the seismic survey. While the same information is present in both the records shot with explosives and the records obtained from vibrator sweeps, there are some differences as well.